Electronic Supplementary Information

Nitrogen-doped Vertical Graphene Nanosheets by High-Flux Plasma Enhanced Chemical Vapor Deposition as Efficient Oxygen Reduction Catalysts for Zn-Air Battery

Zhiheng Wu[a,b], Yongshang Zhang[a,b], Lu Li[a], Yige Zhao*[a], Yonglong Shen*[a,b], Shaobin Wang[c], Guosheng Shao*[a,b]

[a]State Center for International Cooperation on Designer Low-Carbon & Environmental Materials (CDLCEM), 100 Kexue Avenue, Zhengzhou University, Zhengzhou 450001, China

[b]Zhengzhou Materials Genome Institute (ZMGI), Building 2, Zhongyuanzhigu, Xingyang, Zhengzhou 450100, China

[c]School of Chemical Engineering and Advanced Materials, The University of Adelaide, North Terrace, Adelaide, SA 5005, Australia

E-mail: gsshao@zzu.edu.cn, shenyonglong@zzu.edu.cn, zhaoyg@zzu.edu.cn

Supplementary Figures and Tables

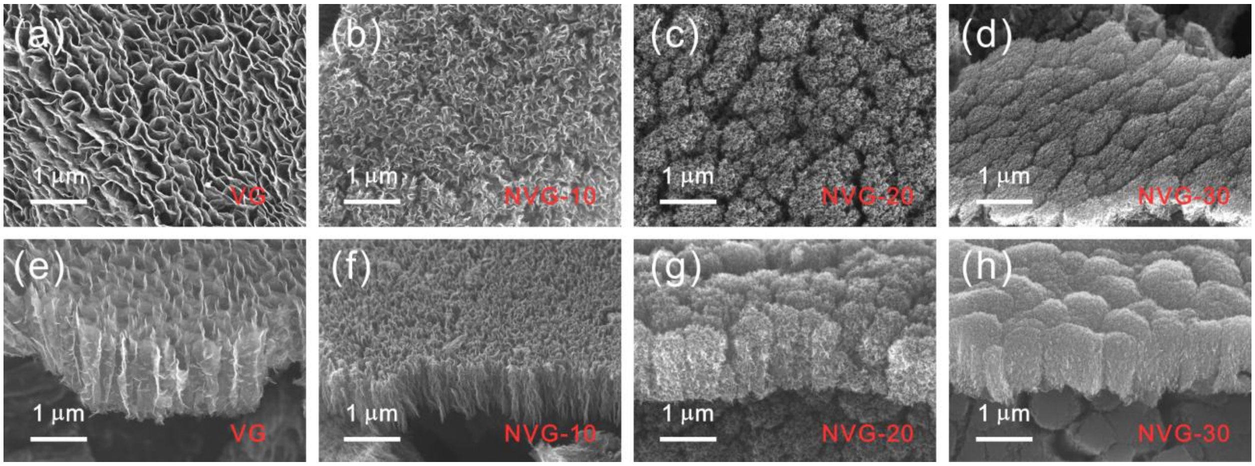

Fig. S1 (a-d) Top view and (e-h) tilted view SEM images of VG, NVG-10, NVG-20 and NVG-30.

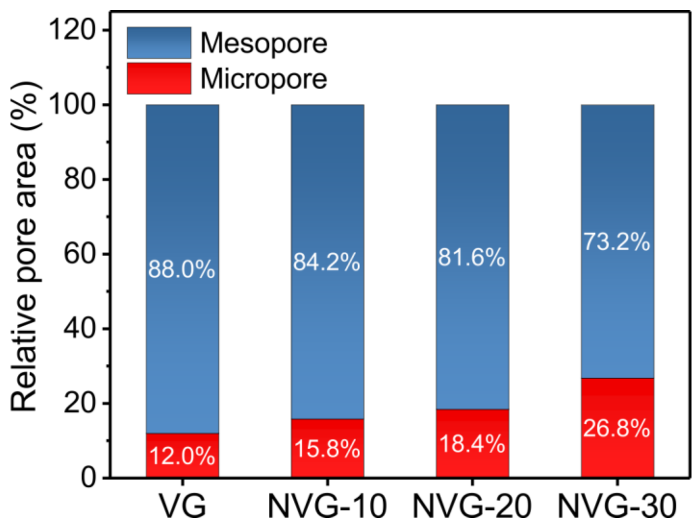

Fig. S2 Relative pore area portions of VG, NVG-10, NVG-20 and NVG-30.

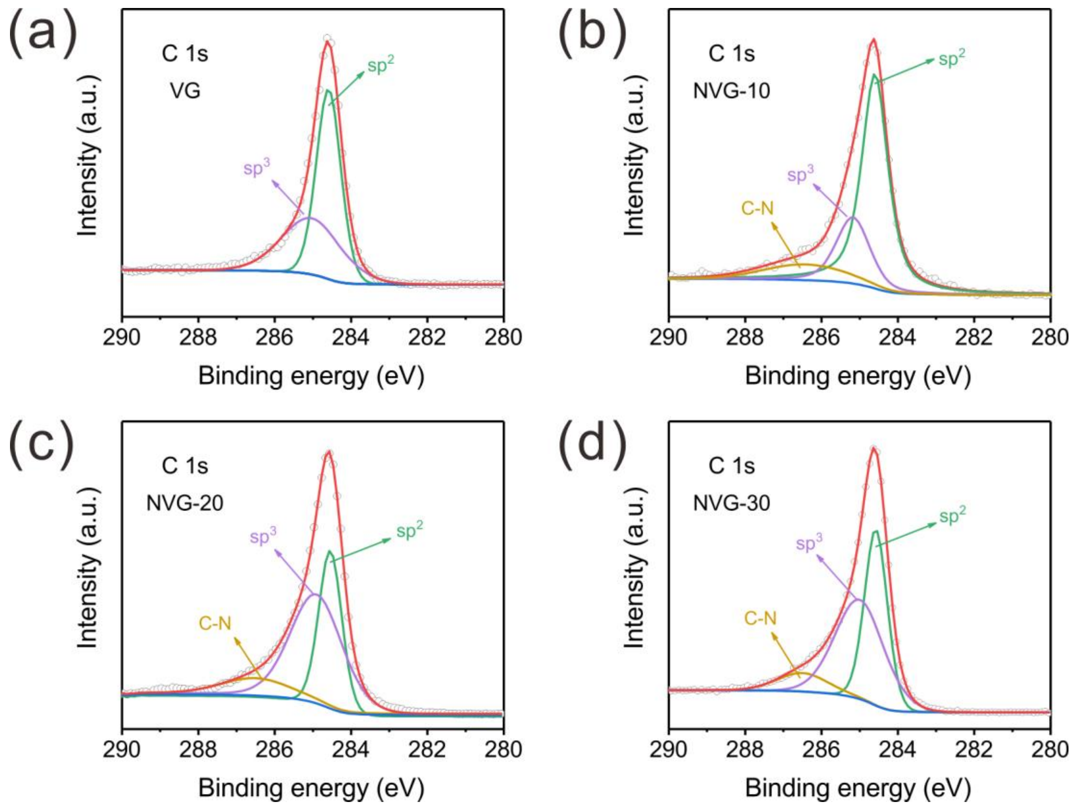

Fig. S3 XPS C 1s scans of (a) VG, (b) NVG-10, (c) NVG-20 and (d) NVG-30.

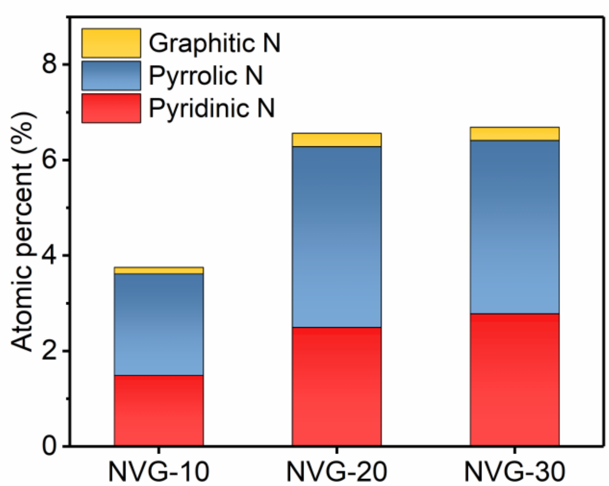

Fig. S4 Contents of nitrogen species of NVG-10, NVG-20 and NVG-30.

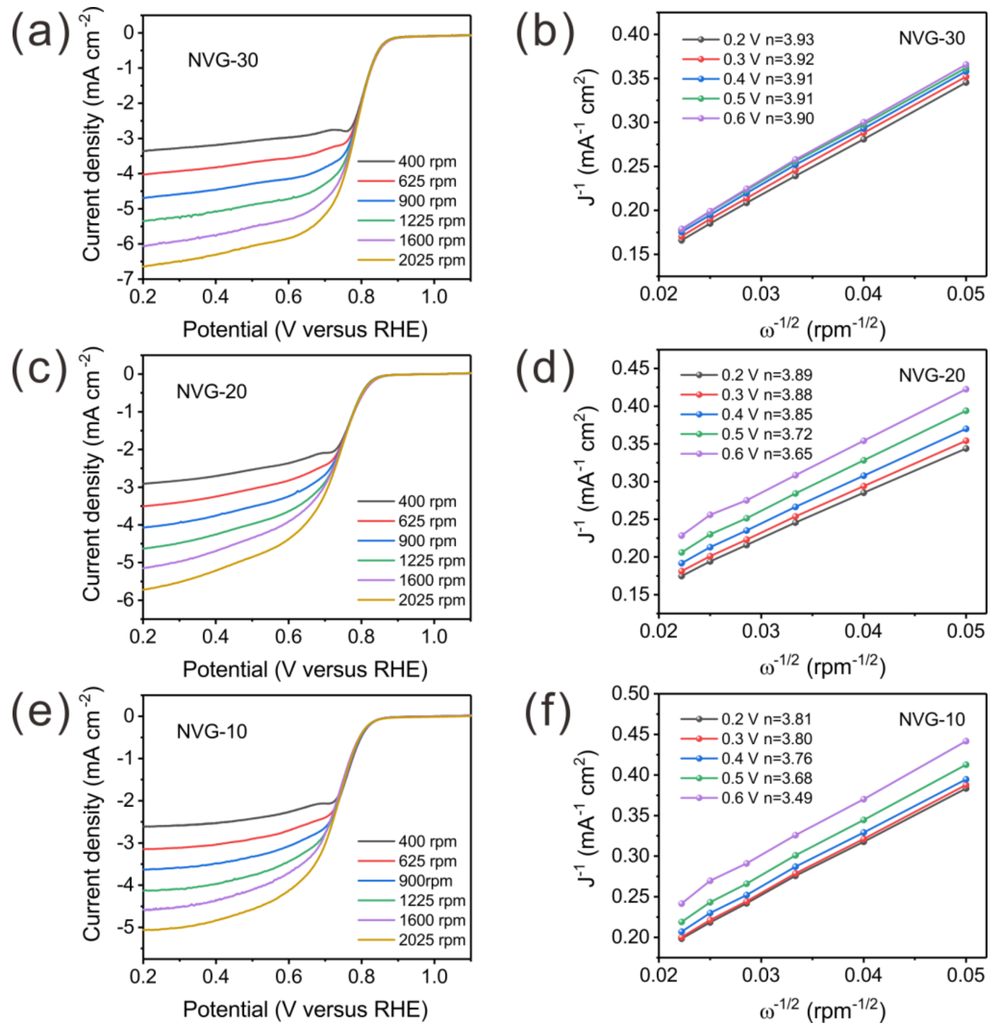

Fig. S5 (a) RDE polarization curves of three NVG samples in O_2-saturated 0.1 M KOH at different rotation speeds; (b) Koutecky-Levich plots (J^{-1} versus $\omega^{-1/2}$) and calculated electron transfer number at different potentials.

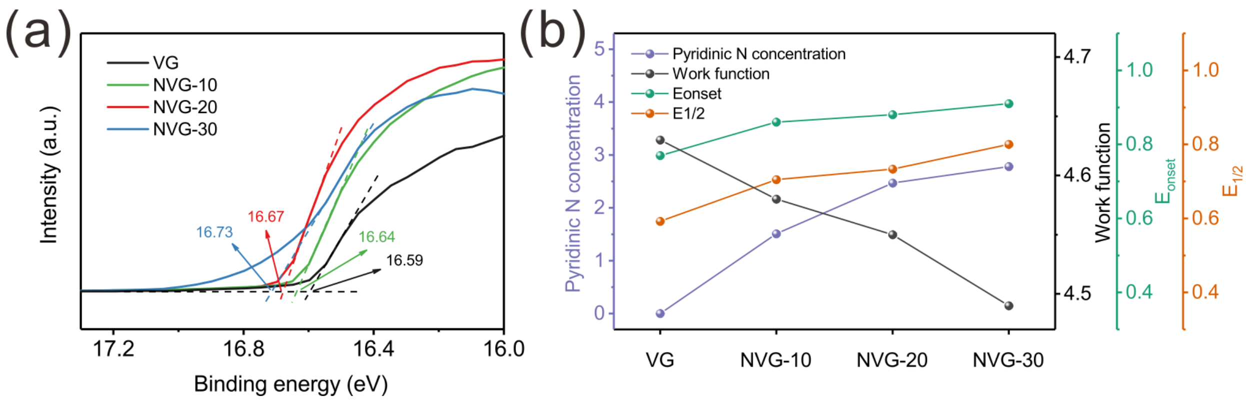

Fig. S6 (a) UPS spectra in the secondary cutoff region of VG and NVG-Xs. (b) Relationship between pyridinic N concentration, work function, E_{onset} and $E_{1/2}$ for VG and NVG catalysts (Lines are guiding eyes).

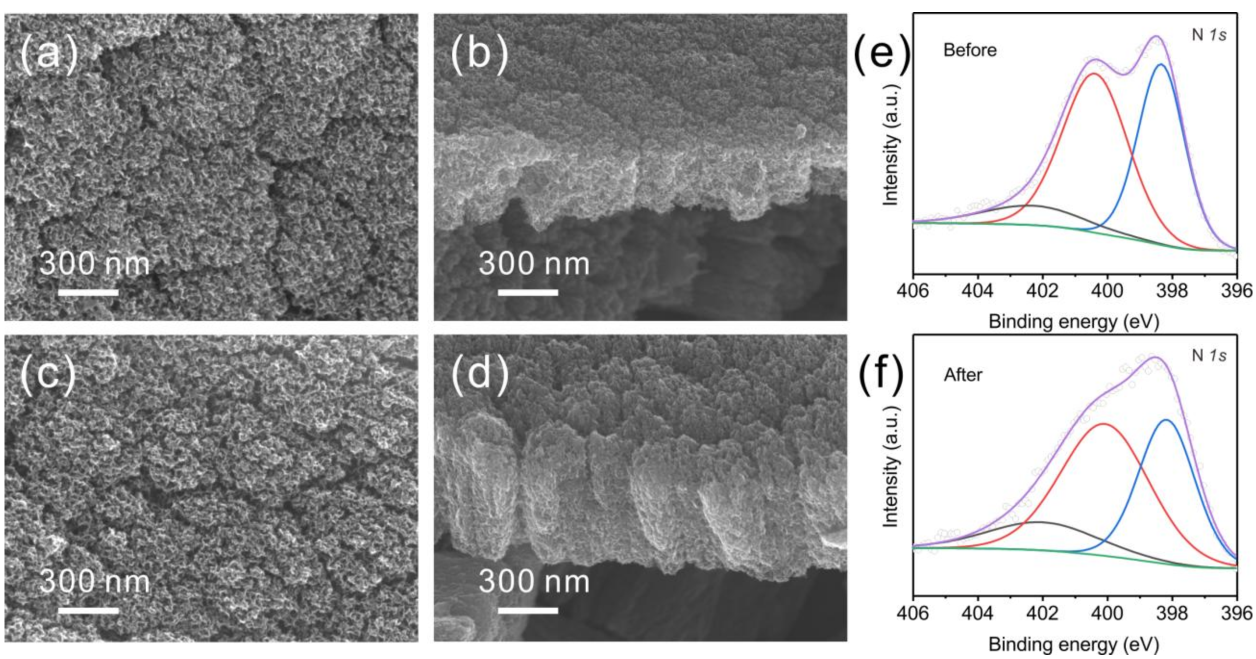

Fig. S7 SEM images of NVG-30 (a-b) before and (c-d) after stability test; (e) and (f) XPS narrow scans of N 1s for NVG-30.

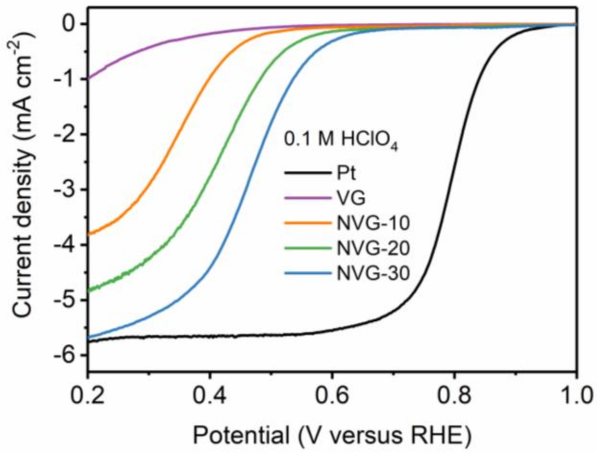

Fig. S8 LSV curves for VG, NVG and commercial Pt/C catalysts in 0.1 M $HClO_4$ solution with a rotation rate of 1600 rpm at 10 mV s^{-1}.

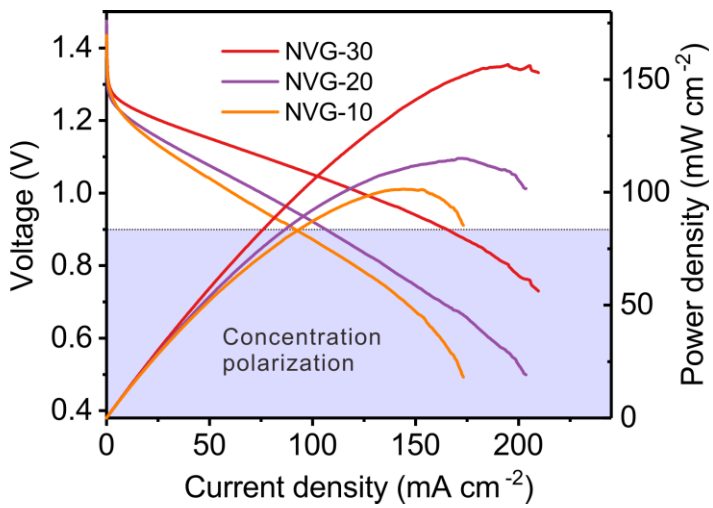

Fig. S9 Discharge polarization curves and the corresponding power density curves of NVG-Xs catalysts.

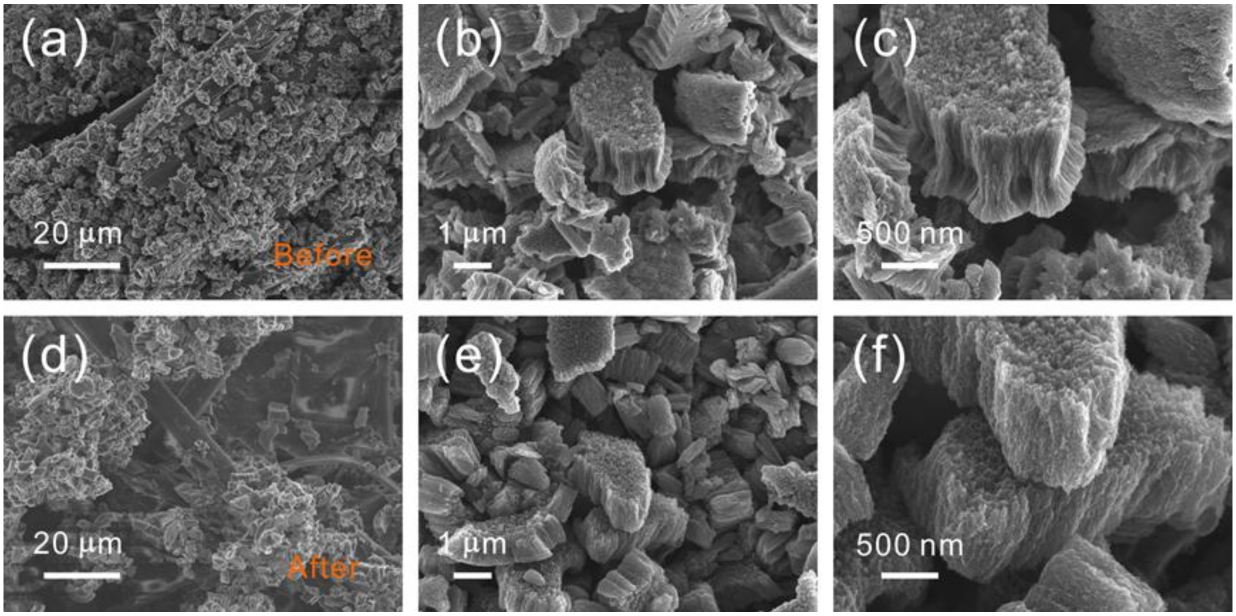

Fig. S10 SEM images of NVG-30 as catalyst layer in Zn-air battery (a - c) before discharge and (d - f) after discharge for 24 h.

Table S1. Pore texture of graphene materials from the DFT pore size distribution measurements.

Sample	Pore area ($m^2\ g^{-1}$)			Pore volume ($cm^3\ g^{-1}$)	
	Micropore	Mesopore	Micropore / (Mesopore + Micropore)	Micropore	Mesopore
VG	4.1	30.2	12.0 %	0.01	0.211
NVG-10	17.4	92.6	15.8 %	0.01	0.488
NVG-20	25.2	111.5	18.4 %	0.025	0.984
NVG-30	64.0	175.1	26.8 %	0.043	1.308

Table S2. Deconvolution of relative compositions of XPS C 1s and N 1s.

Sample	C 1s bond type (%)			N 1s bond type (%)		
	sp^2	sp^3	C-N	pyridinic N	pyrrolic N	graphitic N
VG	58.16	41.84	-	-	-	-
NVG-10	46.77	32.66	20.58	37.66	58.75	3.59
NVG-20	32.54	37.57	26.53	35.98	59.75	4.27
NVG-30	31.97	37.67	30.37	39.55	56.32	4.13

Table S3. Electrocatalytic activities of the recently reported metal-free catalysts for ORR.

Catalyst	Catalyst loading (mg cm^{-2})	E_{onset} (V vs. RHE)	$E_{1/2}$ (V vs. RHE)	j_L (mA cm^{-2})	Reference
NVG-30	**0.47**	**0.91**	**0.80**	**6.3**	**This work**
Nitrogen-doped mesoporous graphene	0.4	0.94	0.83	5.4	Adv. Mater., 2018, 30, 1803588
Nitrogen-doped carbon nanotubes	-	0.88	0.82	5.6	Nano Energy, 2019, 63, 103788
N, S-doped graphene nanoribbons	0.245	0.92	0.78	4.9	Nano Energy, 2019, 66, 104096
B, N-codoped graphene	0.28	0.90	0.69	-	Angew. Chem. Int. Ed., 2013, 52, 3110–3116
N-doped graphene/single-walled CNT hybrids	0.25	0.88	0.63	-	Small, 2014, 10, 2251–2259
N and P co-doped mesoporous nanocarbon	0.15	0.94	0.85	4.0	Nat. Nanotechnol., 2015, 10, 444–452
2D nitrogen-doped carbon nanotubes/graphene hybrid	0.51	0.92	0.85	-	Adv. Funct. Mater., 2020, 30, 1906081
3D honeycombed hierarchical porous N, O-doping carbon	0.256	0.90	0.78	5.3	Appl. Catal. B Environ., 2020, 265, 118603
3D porous N and S co-doped carbon nanosheets	0.13	0.96	0.78	4.3	J. Mater. Chem. A, 2020, 8, 4386–4395
Nitrogen-doped grapheme mesh	0.255	0.89	0.77	6.4	Adv. Mater., 2016, 28, 6845–6851

Table S4. The comparation of electrochemical performance for primary Zn-air batteries based on metal-free catalysts.

ORR Catalyst	Catalyst loading (mg cm^{-2})	Electrolyte	Cell voltage (V)	Peak power Density (mW cm^{-2})	Reference
NVG-30	**1**	**6 M KOH**	**1.24 (5 mA cm^{-2})**	**167.9**	**This work**
nitrogen-enriched carbon nanospheres	1	6 M KOH	1.1 (5 mA cm^{-2})	~160	Energy Storage Mater., 2020, 27, 514–521
N, P, and S-doped graphene-like carbon	1	6 M KOH	1.21 (10 mA cm^{-2})	151	Appl. Catal. B Environ., 2019, 241, 442–451
N-Doped Carbonaceous	2	6 M KOH	-	180	ChemSusChem, 2019, 12, 1017–1025
N and P co-doped mesoporous nanocarbon	0.5	6 M KOH	1.26 (5 mA cm^{-2})	~55	Nat. Nanotechnol., 2015, 10, 444–452
Nanoporous silk-derived N-doped carbon	1	6 M KOH + 0.2 M $Zn(OAc)_2$	0.81 (10 mA cm^{-2})	91.2	Chem. Mater., 2019, 31, 1023–1029
Nano porous carbon nanofiber films	2	6 M KOH + 0.2 M $Zn(OAc)_2$	1.20 (10 mA cm^{-2})	185.0	Adv. Mater., 2016, 28, 3000–3006
N, O-codoped graphene nanorings–integrated boxes	1	6 M KOH + 0.2 M $Zn(OAc)_2$	1.18 (10 mA cm^{-2})	111.9	Adv. Energy Mater., 2019, 9, 1803867
oxygen-modified nitrogen-doped carbon nanosheets	1	6 M KOH	1.1 (10 mA cm^{-2})	89	ACS Appl. Mater. Interfaces, 2018, 10, 11678–11688
N, P-codoped porous carbon spheres	-	6 M KOH + 0.2 M $Zn(OAc)_2$	1.1 (2 mA cm^{-2})	79	Nano Energy, 2019, 60, 536–544

Supplementary note 1

Generally, Pt wire is used as the counter electrode for ORR tests, because of its high stability and availability.[1] Recently, some scientists postulated that Pt may be dissolved under anodic conditions and be transported electrochemically, which may influence the tested electrochemical performance.[2,3] However, the Pt dissolution is related with applied potentials, pH values, transient potential conditions and temperature.[4] So far, the dissolution of Pt and the influence on ORR performance during ORR process have not yet been confirmed, typically in the working potential of 0 < E < 1 V (versus RHE) in strongly alkaline solution. As is realized, many recent studies still adopt Pt as the counter electrode.[5-8]

As a quick test about the possible influence of Pt on the ORR performance for our catalysts, we used a graphite rod as the counter electrode in a three-electrode system to evaluate the ORR activities of VG and NVG-Xs in alkaline solution and the obtained LSV curves are shown as below. We can see that the VG and NVG-Xs catalysts show similar ORR activities using a graphite rod as the counter electrode, to the results measured using a Pt wire as the counter electrode (Figure 3b). This suggests that Pt has little influence on the ORR performance in alkaline solution for our catalysts. As for the ORR tests in acid solution, we used a graphite rod as the counter electrode in order to eliminate the possible disruption about Pt dissolution.

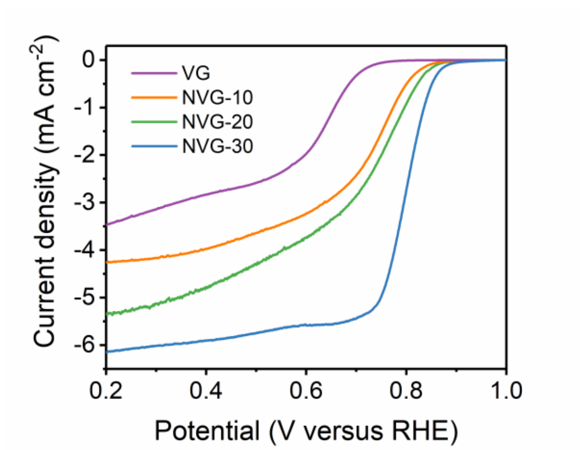

Figure Supplementary note 1 LSV curves for VG, NVG-10, NVG-20 and NVG-30 catalysts in 0.1 M KOH solution using a graphite rod as the counter electrode.

Supplementary References

1 M. B. Stevens, L. J. Enman, A. S. Batchellor, M. R. Cosby, A. E. Vise, C. D. M. Trang and S. W. Boettcher, Chem. Mater., 2017, 29, 120–140.

2 G. Dong, M. Fang, H. Wang, S. Yip, H.-Y. Cheung, F. Wang, C.-Y. Wong, S. T. Chu and J. C. Ho, *J. Mater. Chem. A*, 2015, **3**, 13080–13086.

3 R. Chen, C. Yang, W. Cai, H.-Y. Wang, J. Miao, L. Zhang, S. Chen and B. Liu, *ACS Energy Lett.*, 2017, **2**, 1070–1075.

4 A. A. Topalov, S. Cherevko, A. R. Zeradjanin, J. C. Meier, I. Katsounaros and K. J. J. Mayrhofer, *Chem. Sci.*, 2013, **5**, 631–638.

5 Y. Yuan, J. Wang, S. Adimi, H. Shen, T. Thomas, R. Ma, J. P. Attfield and M. Yang, *Nat. Mater.*, 2020, **19**, 282–286.

6 X. Liu, Y. Yuan, J. Liu, B. Liu, X. Chen, J. Ding, X. Han, Y. Deng, C. Zhong and W. Hu, *Nat. Commun.*, 2019, **10**, 4767.

7 H. Fei, J. Dong, Y. Feng, C. S. Allen, C. Wan, B. Volosskiy, M. Li, Z. Zhao, Y. Wang, H. Sun, P. An, W. Chen, Z. Guo, C. Lee, D. Chen, I. Shakir, M. Liu, T. Hu, Y. Li, A. I. Kirkland, X. Duan and Y. Huang, *Nat. Catal.*, 2018, **1**, 63–72.

8 H. Li, P. Wen, D. S. Itanze, Z. D. Hood, S. Adhikari, C. Lu, X. Ma, C. Dun, L. Jiang, D. L. Carroll, Y. Qiu and S. M. Geyer, *Nat. Commun.*, 2020, **11**, 3928.